Journal of Industrial and Engineering Chemistry 37 (2016) 14–17

Contents lists available at ScienceDirect

Journal of Industrial and Engineering Chemistry

journal homepage: www.elsevier.com/locate/jiec

Short communication

# Effect of bio-template on the properties of $SiO_2/Al_2O_3$ composites for drug delivery

Long-Yue Meng [a], Weiqi Jiang [b], Wenxiang Piao [b], Wan Meng [b,*]

[a] Key Laboratory of Natural Resources of Changbai Mountain and Functional Molecules, Yanbian University, Yanji 133002, China
[b] Department of Chemistry, Yanbian University, Yanji 133002, China

ARTICLE INFO

*Article history:*
Received 6 September 2015
Received in revised form 26 January 2016
Accepted 16 February 2016
Available online 24 February 2016

*Keywords:*
Chitosan
Template
Silica/alumina
Drug delivery
Levofloxacin

ABSTRACT

In this study, $SiO_2/Al_2O_3$ composites (C-SLNs) were successfully synthesized using chitosan as the template for drug delivery. The C-SLNs had higher specific surface areas (244–607 $m^2/g$), total pore volumes (0.19–0.34 $cm^3\,g^{-1}$), and narrow mesopore size distribution. The porosity of the C-SLNs prepared under high Si/Al ratio conditions was achieved mostly by the formation of wider pores that were distributed in the meso-/macro-pores. And, the C-SLNs were used as a levofloxacin carrier to study its drug release behavior, which exhibited an initial fast release followed by a sustained release and antibacterial effectiveness over a long period.



## Introduction

Currently, the development of new, efficient, environmentally safe, cheap, and biodegradable slow/controlled release materials as drug carrier materials in agricultural and pharmaceutical industries is a major challenge. This is particularly important because the innovations and benefits afforded by these delivery systems suggest that developmental focus in this direction will remain to be active for many years to come. However, there are two factors restricting this process. Firstly, ensuring the sustained/controlled release performance of products is a challenge and secondly, the cost of production and ensure that the product is environmentally safe are pertinent issues [1,2].

To date, many different materials have been used as drug carrier materials including polymers (PPC, PVC, PVP, chitosan, etc.), silica, zinc oxide (ZnO), calcium carbonate ($CaCO_3$), and several others [3–7]. In particular, silica nanomaterials have a high potential for application in many areas including as adsorbents, photonics, catalysts, sensors, superhydrophobic surfaces, polymer fillers, and a host of other fields [8–10]. Mesoporous silica has made very significant progress in the past decades as a very important silica nanomaterial in scientific research. This is because of its good biocompatibility, higher specific surface area, adjustable pore size distribution, and the ease of surface modification with different organic groups [11–13]. Furthermore, mixed oxides have attracted more research interest than pure oxides because they have larger specific surface area, higher chemical stability, higher surface acid, and mechanical strength. Among the various mixed oxides, the $SiO_2/Al_2O_3$ mixed oxides, particularly, the mesoporous form, have shown excellent properties including chemical stability, easy availability, reusability, and easy-to-design pore structure [14–16].

Recently, various templates and methods have been developed to improve the morphology, specific surface area, and porosity including the synthesis of mesoporous silica-based nanoparticles. Although different methods have been used to prepare $SiO_2/Al_2O_3$, the sol–gel process is one of best because it controls the morphology of the final materials with a high purity and specificity. Various templates have been used as surfactant in the synthesis of mesoporous materials [17–19].

In particular, chitosan, which is a linear nontoxic bio-polymer with high adsorption properties due to it the presence of hydroxyl and amino groups has been used for this purpose [20,21]. The functional groups present in chitosan make it an excellent candidate to produce hybrid organic–inorganic composite sol–gels, as templates in the presence of acidic oxides. Rajarajeswari et al. [20] used chitosan as a template to synthesize a mesoporous nanotitania photocatalyst. Kadib et al. [22] prepared porous metal oxide microspheres with filamentary nanoparticles using chitosan as a template. Sifontes et al. [23] prepared cerium oxide nanoparticles using chitosan as a template, cerium nitrate as a starting material, and sodium hydroxide as a precipitating agent. Therefore, we proposed that sol–gel synthesis of $SiO_2/Al_2O_3$ using

* Corresponding author. Tel.: +86 0433 273 2340; fax: +86 0433 273 9626.
*E-mail address:* mengw@ybu.edu.cn (W. Meng).

http://dx.doi.org/10.1016/j.jiec.2016.02.012
1226-086X/

chitosan as a template and mesoporous silica-based materials would yield a higher specific surface area. In this study, chitosan was used as a bio-template to prepare mesoporous $SiO_2/Al_2O_3$ composite particles for drug delivery, in an attempt to reduce the cost of raw materials by using environmentally safe and renewable resources.

## Materials and methods

### *Sample preparation*

$SiO_2/Al_2O_3$ composites were prepared according to the following three steps. Firstly, a mixture of tetraethyl orthosilicate (TEOS, 5.6 mL), ethanol ($C_2H_5OH$, 8.7 mL), aluminum nitrate ($Al(NO_3)_3$, 0.75 g, Si/Al = 50), and hydrochloric acid (HCl 0.01 M, 2.7 mL) was stirred at 40 °C for 1 h. The different chitosan/silica ratios ($m_{chitosan}/m_{chitosan\ +\ silica}$ = 0.1 (11.5 mL), 0.2 (25.5 mL), 0.3 (43.5 mL), and 0.4 (68 mL); chitosan molecular weight, $M_w$, 10,000, 1.2 wt%) were dissolved in an acidic solution (2 wt% aqueous acetic acid) and then slowly added to the original TEOS mixture with vigorous stirring at 40 °C for 30 min. The gel obtained was air dried at 25 °C for 5 days in a mold. The transparent composite film was calcined at 550 °C for 2 h. The resultant samples were designated as *G-n*, where *n* is the ratio of $m_{chitosan}/m_{chitosan\ +\ silica}$ (0.1, 0.2, 0.3, and 0.4). To determine the effect of varying the aluminum content on the pore structure of the C-SLNs, different proportions of $Al(NO_3)_3$ were used to prepare a transparent composite gel following steps. A mixture of tetraethyl orthosilicate (TEOS, 5.6 mL), $C_2H_5OH$, (8.7 mL), $Al(NO_3)_3$ (Si/Al = 100 (1.5 g), 150 (2.25 g), and 200 (3 g)), and HCl (0.01 M, 2.7 mL) was stirred at 40 °C for 1 h. The 25.5 mL chitosan (1.2 wt%) were dissolved in an acidic solution (2 wt% aqueous acetic acid) and then slowly added to the 1.5 g TEOS mixture ($m_{chitosan}/m_{chitosan\ +\ silica}$ = 0.2) with vigorous stirring at room temperature for 30 min. The gel obtained was air dried at 25 °C for 5 days in a mold. The transparent composite film was calcined at 550 °C for 2 h. These samples were designated as *H-m*, where *m* is the ratio of Si/Al (100, 150, and 200). In vitro levofloxacin release from the obtained samples was investigated by soaking 10 mg of each material ($SiO_2/Al_2O_3$ composites loaded with drug) in 10 mL of a PBS (phosphate buffer solution, pH = 7.4), in dark conditions at 37 °C with continuous orbital stirring at 100 rpm for 48 h. The amount of levofloxacin released to the PBS was determined by UV spectrophotometry at 293 nm.

### *Characterization*

Nitrogen ($N_2$) adsorption–desorption isotherms were measured using the gas adsorption technique (BET) on a surface area analyzer (Beckman Coulter, SA3100). The morphology of the nanofibers was observed using SEM with a scanning electron microscope (Hitachi S4500) and transmission electron microscopy (TEM, JEOL-2000-FX microscope). The ultraviolet (UV)–visible (Vis) spectra were recorded using a JH754 UV/Vis spectrophotometer (Jinghua Co.).

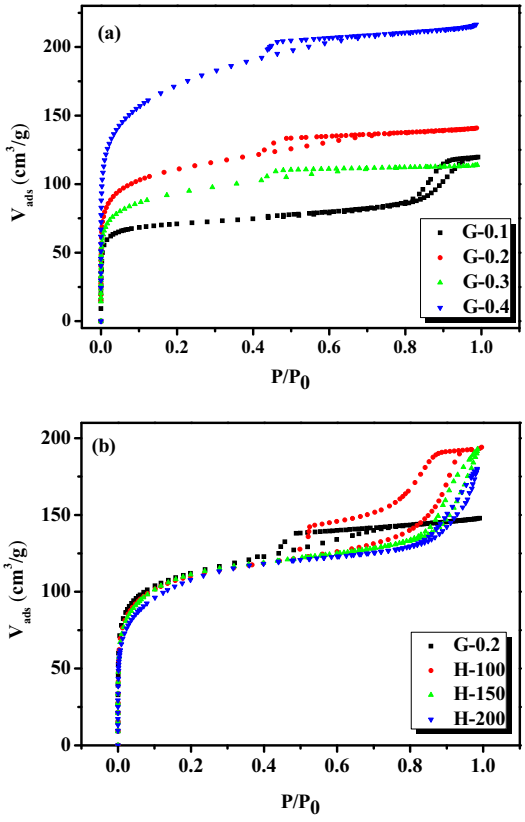


**Fig. 1.** Nitrogen ($N_2$)/77 K full isotherms of the silica/alumina ($SiO_2/Al_2O_3$) nanocomposites (C-SLNs). (a) G-0.1, G-0.2, G-0.3, and G-0.4 transparent film composites; and (b) H-50, H-100, H-150, and H-200 transparent composite gels.

## Results and discussion

To confirm the pore structure of the C-SLNs, we used $N_2$/77 K isotherms, and the results are shown in Fig. 1(a). The adsorption data curves of the samples show that they are type-IV isotherms, according to the International Union of Pure and Applied Chemistry (IUPAC) classification. The comparison of all the sample curves shows that the chitosan template promoted the development of micro-/mesoporosity, by the air calcination of the template at 550 °C. The adsorption capacity increased significantly with increasing chitosan content. This suggests that samples produced with the chitosan template are composed mainly of mesopores. Fig. 1(b) shows the change in the shape of the isotherms ($P/P_0$ range, 0.4–1) with increasing Si/Al ratio from 50 to 200, indicating the main changes in the mesopore structure of the prepared C-SLNs. This suggests that samples produced at low Si/Al ratios are composed mainly of mesopores, and those synthesized at high chitosan/chitosan-silica (C/CS) ratios are composed mainly of micro/mesopores [20–24].

Table 1 provides the details of the textural properties of the prepared C-SLNs. The micropore, mesopore, and total pore

**Table 1**
Textural properties of the silica/alumina ($SiO_2/Al_2O_3$) composites (C-SLNs).

| Sample | $S_{BET}$ ($m^2$/g) | $S_{MicroBET}$ ($m^2$/g) | $V_{Mi}$ (mL/g) | $V_{Me}$ (mL/g) | $V_T$ (mL/g) | $V_{Me}/V_T$ (%) |
|---|---|---|---|---|---|---|
| G-0.1 | 244 | 188 | 0.085 | 0.105 | 0.190 | 55.3% |
| G-0.2 | 384 | 228 | 0.098 | 0.122 | 0.220 | 55.4% |
| G-0.3 | 431 | 247 | 0.101 | 0.149 | 0.250 | 59.6% |
| G-0.4 | 607 | 275 | 0.120 | 0.230 | 0.350 | 67.6% |
| H-100 | 389 | 214 | 0.094 | 0.206 | 0.300 | 69.0% |
| H-150 | 395 | 200 | 0.086 | 0.204 | 0.290 | 70.3% |
| H-200 | 385 | 146 | 0.061 | 0.219 | 0.280 | 78.2% |

volumes, as well as the specific surface area, mesopore volume ratio, and average pore diameter of the C-SLNs were estimated from the $N_2$/77 K adsorption isotherms. Increasing the C/CS ratio from 0.1 to 0.4 increased the specific surface area and total pore volume significantly from 244 to 607 $m^2/g$ and 0.19 to 0.34 $cm^3\,g^{-1}$, respectively. The results conclude that the pore size distribution range of the $SiO_2/Al_2O_3$ composite is narrow and that the pore diameters tend to become homogeneous. However, the micro specific surface area, micropore volume, and total pore volume decreased with increasing Si/Al ratio up to 200, while the mesopore volume increased from 0.133 to 0.219 $cm^3\,g^{-1}$. The porosity of the C-SLNs prepared under high Si/Al conditions was achieved mostly by the formation of wider pores that were distributed in the meso-/macropores. It further proved that the $SiO_2/Al_2O_3$ molar ratio resulted in the destruction of microporous structure of C-SLNs formed in the following sol–gel process.

For clearer characterization of the change in the pore structure of the prepared C-SLNs studied, Fig. 2 presents the pore size distribution in the mesopore region. The mesopore size distributions of the prepared C-SLNs at different carbonization temperatures were determined using the Barrett–Joyner–Halenda (BJH) methods. As shown in Fig. 2(a), the micropore structures were enhanced when chitosan was used as the template, whereas the distributions revealed a slight development around the mesopore region (2–6 nm) with increasing C/CS ratio. Fig. 2(b) shows that the pore size of the C-SLNs prepared by changing the Si/Al ratios from 50 to 200, had a wider range distribution of 2–60 nm, which increased with increasing Si/Al ratio in the bigger mesopores (10–20 nm). This could be responsible for corresponding enhanced porosity related to the extra-structure porosity and interparticle spacing. The results illustrated in Fig. 2(b) also show that a larger content of $Al_2O_3$ in the C-SLNs decreased the volume and size of the pores, thereby changing the hysteresis profile [14].

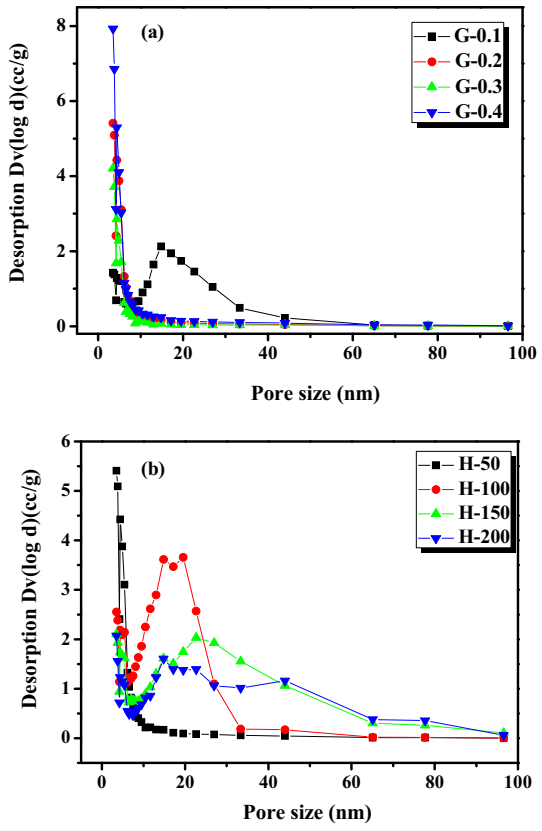


**Fig. 2.** Mesopore size distributions of silica/alumina ($SiO_2/Al_2O_3$) nanocomposites (C-SLNs). (a) G-0.1, G-0.2, G-0.3, and G-0.4 transparent film composites; and (b) H-50, H-100, H-150, and H-200 transparent gel composites.

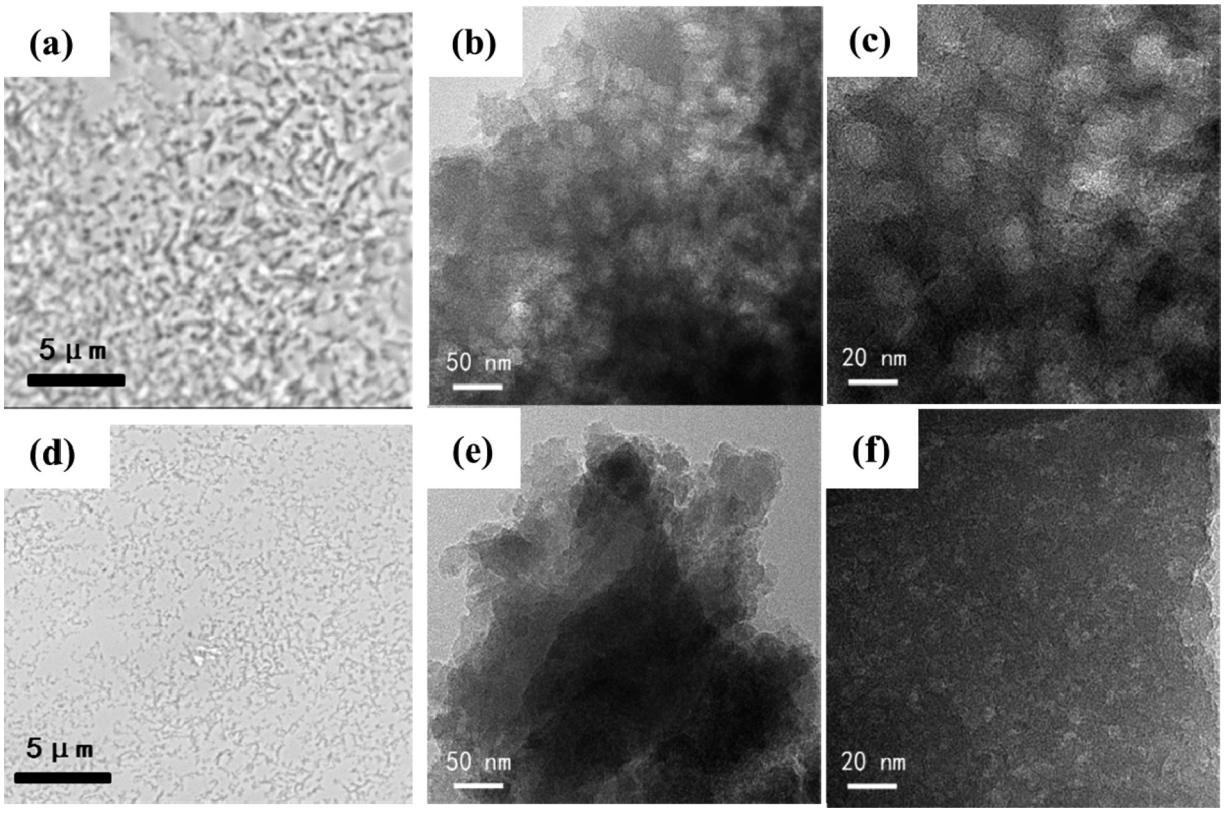


**Fig. 3.** SEM (a, d) and TEM (b, c, e, f) images of silica/alumina ($SiO_2/Al_2O_3$) nanocomposites (C-SLNs) formulated with transparent film composites G-0.1 (a, b, c) and G-0.4 (d, e, f).

Fig. 3 shows the SEM and TEM images of the template-free porous silica products synthesized with C/CS ratio of 0.1 and 0.4. Similar to the explanation proposed for the BJH pore diameter, the pore size of the C-SLNs clearly decreased with increasing C/CS ratios. Fig. 3(c) and (f) shows the bimodal pore structure of the silica products synthesized with the chitosan template at C/CS ratio 0.1 and 0.4, which consisted of wormhole-like mesopores (2–10 nm) and macropores (100 nm) caused by removal of the template during the calcination process [20–22]. In addition, the SEM images (Fig. 3(d)) show that the $SiO_2/Al_2O_3$ composites exhibit a significant homogeneous pore structure with diameters in the range of approximately 100–70 nm, which indicates that chitosan content increases the uniformity of the composite via a structural adjustment of silica particles.

Usually, the drug release from the nanoparticles depends on the location of the drug molecules in the nanoparticles, the interaction between the drug and the polymer, and the properties of the carrier materials. The drug release pathways include the following pathways: (1) The drug desorption release. The drug is binds to the surface of the nanoparticles, and the release of the drug can be achieved through desorption, which usually produce burst release; (2) The diffusional release. It means that release media through the surface of the nanoparticles into the inside of the micropores and then drug dissolution and diffusion into the media. (3) Dissolution or degradation of the pharmaceutical carrier. When the binding force of the carrier material and the drug molecule is larger, the drug release is carried out by layer by layer dissolution or degradation of the nanoparticles, and the release rate is controlled by the dissolution or the degradation rate of the carrier.

In vitro stability studies were performed to elucidate the different initial release profiles of the prepared C-SNLs (Fig. 4). As can be seen, all the release profiles show a slow release rate at the beginning followed by a slower one with increased time until the equilibrium is attained. In detail for C-SNLs, the amount of drug release from G-0.1, G-0.2, G-0.3; and G-0.4 systems was 34.0, 25.0 26.1 wt%, and 35.8 wt% within 40 h, respectively. And all of the levofloxacin release from C-SNLs within 100 h. As expected, the G-0.1 underwent rapid dissolution, with 100% release of levofloxacin after approximately 100 h. For sample G-0.2 and G-0.3, the drug release rate reaching 43.46 wt% at 40 h, the burst release phenomenon is serious; and then the drugs within 80 h release a quantity to 56.17 wt%, subsequent release gradually slowed down, which shows a significant sustained-release effect; the release of the drug gradually slow is smooth release after 120 h. It indicates that there is a strong interaction between the drug and the C-SNLs. The results can speculate that some of the drugs may be adsorbed on the surface of the C-SNLs due to the weak binding force after entering the release medium, and the combination of drug and C-SNLs is broken, which will cause in the emergence of the initial stage of burst release phenomenon. The G-0.4 with the highest C/CS ratio, exhibited delayed release characteristics, and about 90% levofloxacin was released after 50 h [25,26]. It reported that, initial burst release rate was affected by the change of pore volume. When the pore volume increased, the initial burst release rate increased; this may be due to the higher concentration of drug presence in the micro-/meso-pore of C-SNLs.

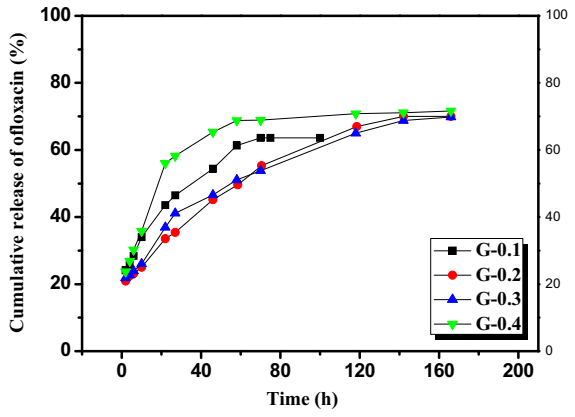


**Fig. 4.** Cumulative release of levofloxacin from silica/alumina ($SiO_2/Al_2O_3$) nanocomposites (C-SLNs) formulated with G-0.1, G-0.2, G-0.3, and G-0.4 transparent film composites.

## Conclusions

In summary, we successfully prepared chitosan-templated $SiO_2/Al_2O_3$ particles for drug delivery and the results showed they had higher specific surface areas (244–607 $m^2/g$) and total pore volumes (0.19–0.34 $cm^3\ g^{-1}$), as well as narrow mesopore size distribution. The chitosan influenced the particle size and pore dimensions by a Lewis base type interaction with the acidic sites on silica and alumina. And, the porosity of the C-SLNs prepared under high Si/Al ratio conditions was achieved mostly by the formation of wider pores that were distributed in the meso-/macro-pores. In vitro release studies showed that the C-SLNs exhibited an initial fast release followed by a sustained release, which was maintained along with sustained antibacterial efficacy for the study duration. These results suggest that the levofloxacin-loaded cross-linked chitosan-templated micro-/meso-pores can be used as a bio-carrier for both oral and implant drug delivery applications, and the drug release was attributed to the formation of micro-/meso-pores.

## Acknowledgements

This study was supported by Gant No. 51163016, from the National Science Foundation of China.

## References

[1] S. Mura, J. Nicolas, P. Couvereur, Nat. Mater. 12 (2013) 991.
[2] P.L. Lee, W.R. Good (Eds.), Controlled-release Technology, ACS Symposium Series, vol. 348, Ciba-Geigy Corporation, Ardsley, NY, 1987, p. 1 (Chapter 1).
[3] Y.Y. Li, F. Cunin, J.R. Link, T. Gao, R.E. Betts, S.H. Reiver, V. Chin, S.N. Bhatia, M.J. Sailor, Science 28 (2013) 2045.
[4] C. Jia, J. Song, Y. Jin, O.J. Rojas, Appl. Polym. Sci. 132 (2015) 42562.
[5] H. Peng, B. Cui, G. Li, Y. Wang, N. Li, Z. Chang, Y. Wang, Mater. Sci. Eng. 46 (2015) 253.
[6] D. Volodkin, Adv. Colloid Interface Sci. 207 (2014) 306.
[7] A.R. Solanki, B.V. Kamath, S.J. Thakore, Appl. Polym. Sci. 132 (2015) 42223.
[8] L.Y. Meng, S.Y. Han, N.Z. Jiang, W. Meng, Mater. Chem. Phys. 148 (2014) 798.
[9] L.Y. Meng, K.Y. Rhee, S.J. Park, J. Ind. Eng. Chem. 20 (2014) 1672.
[10] R. Selvaggi, L. Tarpani, A. Santuari, S. Giovagnoli, L. Latterini, Appl. Catal. B: Environ. 168–169 (2015) 363.
[11] C. Ma, L. Tarpani, Z. Huang, J. Feng, Y. Yao, S. Chen, Chem. Mater. 23 (2011) 3583.
[12] G. Yang, S. Gai, F. Qu, P. Yang, ACS Appl. Mater. Interfaces 5 (2013) 5788.
[13] F. Mahdizadeh, M.J. Eskandarian, Ind. Eng. Chem. 20 (2014) 2378.
[14] J. Godnjavec, J. Zabret, B. Znoj, S. Skale, N. Veronovski, P. Venturini, Prog. Org. Coat. 77 (2014) 47.
[15] A. Nazari, S. Riahi, Energy Build. 43 (2011) 2939.
[16] J. Wang, J. Li, Y. Wang, G. Luo, Chem. Eng. J. 236 (2014) 293.
[17] T. Li, Z. Shu, J. Zhou, Y. Chen, D. Yu, X. Yuan, Y. Wang, Appl. Clay Sci. 107 (2015) 182.
[18] Y. Li, B. Li, Z. Yan, Z. Huang, K. Hu, S. Wang, Y. Yang, Chem. Mater. 25 (2013) 307.
[19] Y. Zhang, X. Liu, J. Huang, ACS Appl. Mater. Interfaces 3 (2011) 3272.
[20] T. Preethi, B. Abarna, G.R. Rajarajeswari, Appl. Surf. Sci. 319 (2014) 197.
[21] T. Preethi, B. Abarna, G.R. Rajarajeswari, Appl. Surf. Sci. 317 (2014) 90.
[22] A.E. Kadib, K. Molvinger, T. Cacciaguerra, M. Bousmina, D. Brunel, Micropor. Mesopor. Mater. 142 (2011) 301.
[23] A.B. Sifontes, G. Gonzalez, J.L. Ochoa, L.M. Tovar, T. Zoltan, E. Cañizales, Mater. Res. Bull. 46 (2011) 1794.
[24] T. Witoon, M. Chareonpanich, J. Limtrakul, Mater. Lett. 62 (2008) 1476.
[25] J. He, A. Zhang, Y. Zhang, Y. Guan, Macromolecules 44 (2011) 2245.
[26] Y. Wang, Q. Zhao, N. Han, L. Bai, J. Li, J. Liu, E. Che, L. Hu, Q. Zhang, T. Jiang, S. Wang, Nanomed.: NBM 11 (2015) 313.